ISH Journal of Hydraulic Engineering

ISSN: 0971-5010 (Print) 2164-3040 (Online) Journal homepage: http://www.tandfonline.com/loi/tish20

Short-term and long-term streamflow prediction by using 'wavelet–gene expression' programming approach

Sepideh Karimi, Jalal Shiri, Ozgur Kisi & Abbas Ali Shiri

To cite this article: Sepideh Karimi, Jalal Shiri, Ozgur Kisi & Abbas Ali Shiri (2016) Short-term and long-term streamflow prediction by using 'wavelet–gene expression' programming approach, ISH Journal of Hydraulic Engineering, 22:2, 148-162, DOI: 10.1080/09715010.2015.1103201

To link to this article: http://dx.doi.org/10.1080/09715010.2015.1103201

ISH JOURNAL OF HYDRAULIC ENGINEERING, 2016
VOL. 22, NO. 2, 148–162
http://dx.doi.org/10.1080/09715010.2015.1103201

Taylor & Francis
Taylor & Francis Group

Short-term and long-term streamflow prediction by using 'wavelet–gene expression' programming approach

Sepideh Karimi[a], Jalal Shiri[a], Ozgur Kisi[b] and Abbas Ali Shiri[c]

[a]Water Engineering Department, Faculty of Agriculture, University of Tabriz, Tabriz, Islamic Republic of Iran; [b]Civil Engineering Department, Canik Basari University, Samsun, Turkey; [c]Department of Civil Engineering, Islamic Azad University, Marageh Branch, Marageh, Islamic Republic of Iran

ABSTRACT

Forecasting short-term and long-term streamflows is of most importance for analyzing water resources systems as well as for many other hydrological applications. In this study, a new combination method (wavelet–genetic programming) was proposed for predicting short-term and long-term streamflows. The new combination method combines the discrete wavelet transform and genetic programming methods to forecast streamflow. The results obtained showed very high agreement between the observed and modeled values. The combination models are compared with the auto regressive moving average and the classic artificial intelligences methodologies, including neuro-fuzzy system and neural networks. The benchmark results show that the new wavelet–genetic programming methodology surpasses all of the other applied models for predicting short-term and long-term streamflows.

ARTICLE HISTORY
Received 16 May 2015
Accepted 6 September 2015

KEYWORDS
Streamflow; wavelet transform; genetic programming; neuro-fuzzy; neural networks

1. Introduction

Streamflow forecasting is an important issue in many hydrology and water resources activities associated with the planning and operation of the water resources components, for allocating water supplies optimally (for competing water users) and for providing information about the sediment amount carried in a river (Kisi 2007a). There are many parameters (e.g., precipitation, evapotranspiration, groundwater level fluctuation, antecedent moisture content of the soil) which affect the next day runoff (Kisi 2008). Although it is possible to identify sophisticated models taking into consideration, the hydrological and hydro-meteorological variables such as precipitation, evapotranspiration, runoff and temperature, it will be economically preferable that a model which simulates the streamflow variations based on previously recorded flow amounts be available for research as well as practical purposes, as discussed by Kisi (2008). Therefore, the current work applies the previously recorded streamflow values as inputs for models to forecast streamflow values in some forecast horizons. This article aims at demonstrating the abilities of hybrid wavelet–genetic programming (WGEP) model to forecast streamflows, based on previously measured flow values and comparing the results with those obtained using genetic programming (GP), adaptive neuro-fuzzy inference system (ANFIS), artificial neural networks (ANN) and auto regressive moving average (ARMA) models.

In the recent past, the use of artificial intelligence (AI) has received more attention in water resources engineering (e.g., ASCE 2000a,b; Coulibaly et al. 2001; Kisi 2006a,b; Kisi 2007b; Maier and Dandy 2000; Minnes and Hall 1996; Shiri and Kisi 2010, 2011; Supharatid 2003; Tayfur 2002). Under AI context, the effective data driving models e.g., ANFIS, ANN, and GP have attracted more attention due to their advantages. Review of all research carried out with AI in water resources engineering is beyond the scope of this article and we will review only studies associated with applications of AI for streamflow modeling. Nayak et al. (2004) applied neuro-fuzzy technique for modeling streamflow time series. Huang et al. (2004) applied ANN for forecasting streamflow in Apalachicola River, US. Wang et al. (2006) employed hybrid ANN models for forecasting daily streamflow. Jain and Kumar (2007) applied hybrid ANN model for forecasting monthly streamflow time series. Kisi (2008) compared different neural network techniques for estimating river flows.

An ANFIS is a combination of an adaptive neural network and a fuzzy inference system (FIS). The parameters of the FIS are determined by the NN learning algorithms. Since this system is based on the FIS, reflecting amazing knowledge, an important aspect is that the system should be always interpretable in terms of fuzzy IF-THEN rules. ANFIS is capable of approximating any real continuous function on a compact set to any degree of accuracy (Jang et al. 1997). ANFIS identifies a set of parameters through a hybrid learning rule combining back propagation gradient descent error digestion and a least square error method. There are largely two approaches for FISs, namely the approaches of Mamdani and Assilian (1975) and Takagi and Sugeno (1985). The differences between these two approaches arise from the consequent part where Mamdani's approach uses fuzzy membership functions (MFs), while linear or constant functions are used in the Sugeno's approach. The neuro-fuzzy model used in this study implements the Sugeno's fuzzy approach (Takagi and Sugeno 1985) to obtain the values for the output variable from those of input variables. The input parameters of the applied ANFIS model in the present investigation are the previously streamflow records where as the streamflows in following 1-, 2-, and 3-days are the ANFIS outputs.

CONTACT Jalal Shiri jalalshiri@tabrizu.ac.ir

GP was first proposed by Koza (1992), as a generalization of genetic algorithms (GAs) (Goldberg 1989) and is particularly suitable where interrelationships among the relevant variables are poorly understood; a theoretical analysis is constrained by assumptions and therefore their solutions are of limited use; and there is a large amount of data in computer readable forms requiring tedious processing. Owing to these restrictions, it is justifiable to test the applicability of GP to model pan evaporation rates in terms of directly measured independent variables of air temperature, sunshine hours, wind speed, and relative humidity.

In the last decade, wavelet transform has become a useful technique for analyzing variations, periodicities and trends in the time series. Smith et al. (1998) used a discrete wavelet transform (DWT) for quantifying streamflow variability. Lu (2002) applied wavelet transform for decomposition of inter-decadal and inter-annual components of rainfall data in rainy season. Xingang et al. (2003) investigated the rainfall spectrum and its evolution of North China in rainy season with summer monsoon decaying inter-decadal time scale using wavelet analysis. Coulibaly and Burn (2004) used wavelet analysis to identify and describe variability in annual Canadian streamflows and to gain insights into the dynamical link between the streamflows and the dominant modes of climate variability in the Northern Hemisphere. Labat (2005) reviewed the most recent wavelet applications in the field of earth sciences and illustrated new wavelet analysis methods in the field of hydrology. Labat et al. (2005) demonstrated that the application of new wavelet indicators (combined continuous and multi-resolution analysis, wavelet entropy, wavelet coherence, wavelet cross-correlation) leads to several improvements in the analysis of global hydrological signal (ENSO, SOI, NAO, SAO) fluctuations and of their mutual time varying relationships. Partal and Kucuk (2006) used a DWT for determining the possible trends in annual total precipitation series. Partal and Kisi (2007) proposed a new combination model (wavelet–neuro-fuzzy) for precipitation forecast. Zhou et al. (2008) proposed a wavelet predictor-corrector model for the simulation and prediction of monthly discharge time series. Kisi (2009) introduced the wavelet–ANN combination model for forecasting intermittent streamflow. Shiri and Kisi (2010) developed and tested a wavelet–neuro-fuzzy model for forecasting short-term and long-term streamflows. Kisi and Shiri (2011) developed wavelet–ANFGIS and wavelet–GP models for rainfall forecasting. Kisi and Shiri (2012) developed wavelet–ANFIS models of short-term groundwater level fluctuation forecasting. Nourani and Andalib (2015) developed wavelet-based AI methods of sediment prediction.

2. Methods

2.1. Discrete wavelet transform

Wavelet function $\psi(t)$ called the mother wavelet can be defined as $\int_{-\infty}^{+\infty} \psi(t)\,\mathrm{d}t = 0$. $\psi_{a,b}(t)$ can be obtained through compressing and expanding $\psi(t)$:

$$\psi_{a,b}(t) = |a|^{-1/2}\psi\left(\frac{t-b}{a}\right) \quad b \in R, a \in R, a \neq 0 \qquad (1)$$

where $\psi_{a,b}(t)$ = the successive wavelet, a = scale or frequency factor, b = a time factor; R = the domain of real numbers.

If $\psi_{a,b}(t)$ satisfies Equation (1), for the time series $f(t) \in L^2(R)$ or finite energy signal, successive wavelet transform of $f(t)$ is defined as:

$$W_\psi f(a,b) = |a|^{-1/2}\int_R f(t)\overline{\psi}\left(\frac{t-b}{a}\right)\mathrm{d}t \qquad (2)$$

where $\bar{\psi}(t)$ = complex conjugate functions of $\psi(t)$. It can be seen from Equation (2) that the wavelet transform is the decomposition of $f(t)$ under different resolution levels (scale). In other words, to filter wave for $f(t)$ with different filters is the essence of wavelet transform.

The successive wavelet is often discrete in real applications. Let $a = a_0^j$, $b = kb_0a_0^j$, $a_0 > 1$, $b_0 \in R$, k, j are integer numbers. DWT of $f(t)$ can be written as

$$W_\psi f(j,k) = a_0^{-j/2}\int_R f(t)\overline{\psi}\left(a_0^{-j}t - kb_0\right)\mathrm{d}t \qquad (3)$$

The most common (and simplest) choice for the parameters a_0 and b_0 is 2 and 1 time steps, respectively. This power of two logarithmic scaling of the time and scale is known as dyadic grid arrangement and is the simplest and most efficient case for practical purposes (Mallat 1989). Equation (3) becomes binary wavelet transform when $a_0 = 2$, $b_0 = 1$:

$$W_\psi f(j,k) = 2^{-j/2}\int_R f(t)\overline{\psi}\left(2^{-j}t - k\right)\mathrm{d}t \qquad (4)$$

The characteristics of the original time series in frequency (a or j) and time domain (b or k) at the same time are reflected by $W_\psi f$ (a, b) or $W_\psi f$ (j, k). When the frequency resolution of wavelet transform is low, but the time domain resolution is high, a or j becomes small. When the frequency resolution of wavelet transform is high, but the time domain resolution is low, a or j becomes large (Wang and Ding 2003).

For a discrete time series $f(t)$, where occurs at different time t (i.e., here integer time steps are used), the DWT can be defined as:

$$W_\psi f(j,k) = 2^{-j/2}\sum_{t=0}^{N-1} f(t)\,\overline{\psi}\left(2^{-j}t - k\right) \qquad (5)$$

where $W_\psi f(j,k)$ is wavelet coefficient for the discrete wavelet of scale $a = 2^j$, $b = 2^jk$.

DWT operates two sets of function viewed as high-pass and low-pass filters. The original time series are passed through high-pass and low-pass filters and separated at different scales. The time series is decomposed into one comprising its trend (the approximation) and one comprising the high frequencies and the fast events (the detail) (Kisi 2009). In this study, the detail coefficients and approximation (A) sub-time series are obtained using the Equation (5).

2.2. Gene expression programming

One of the strong points of the gene expression programming (GEP) approach is that the creation of genetic diversity is extremely simplified as genetic operators work at the chromosome level. Another strong point is that GEP consists of its unique, multigenic nature which allows the evolution of more complex programs composed of several subprograms. As

a result, GEP surpasses the old GP system in 100–10,000 times (Ferreira 2001). The advantages of a system-like GEP are clear from its nature, but the most important are (Ferreira 2002): (i) the chromosomes are simple entities: linear, compact, relatively small, easy to manipulate genetically (replicate, mutate, recombine, etc.); (ii) the expression trees are exclusively the expression of their respective chromosomes; they are entities upon which selection acts, and according to fitness, they are selected to reproduce with modification.

According to Ferreira (2006), GEP is like GAs and GP, a genetic algorithm as it uses populations of individuals, selects them according to fitness, and introduces genetic variation using one or more genetic operators.

In general, selection of input variables does not completely define the environment from which the system will learn. One must also choose specific past examples from the learning domain. Each example should contain data that represent one instance of the relationship between the chosen inputs and outputs. These examples are referred to as "training cases" while they are called "fitness cases" in GP. Once the training set is selected, one can say that the learning environment of the system is defined (Banzhaf et al. 1998).

The procedure of streamflow forecasting is as follows: The first step is the selection of fitness function. For this problem, the root relative squared error (RRSE) fitness function, E_i, of an individual program, i, was applied (Ferreira 2006):

$$E_i = \sqrt{\frac{\sum_{j=1}^{n}\left(P_{ij} - T_j\right)^2}{\sum_{j=1}^{n}\left(T_j - \bar{T}\right)^2}} \tag{6}$$

where $P_{i,j}$ is the value predicted by individual program i for fitness case j, and T_j is the target value for fitness case j and $\bar{T}$ is computed by the following formula:

$$\bar{T}_j = \frac{1}{n}\sum_{j=1}^{n} T_j \tag{7}$$

For a perfect fit, $E_i = 0$. It should be, however, noted that the term E_i cannot be applied as fitness function directly, since it does not increase with increasing the program performance, proportionally. Therefore, for evaluating the fitness f_i of an individual program i, the following equation should be applied

$$f_i = 1000\,\frac{1}{1+E_i} \tag{8}$$

which obviously ranges between 0 and 1000 with 1000 corresponded to the ideal (Ferreira 2006). The second step consists of choosing the set of terminals T and the set of functions F, to create the chromosomes. In the current problem, the terminal set includes recorded streamflow values: $\{Q_{t-3}, Q_{t-2}, Q_{t-1}, Q_t\}$, where Q_i represents the streamflow at ith time step. The study examined the various combinations of these parameters as inputs to the GEP models. The choice of the appropriate function depends on the viewpoint of user. In this study, different mathematical functions were utilized ($\{+, -, *, /\}$, $\{\sqrt{}, \sqrt[3]{}, \ln(x), e^x, x^2, x^3, \sin(x), \cos(x), \text{arctg}(x)\}$). The third step is to choose the chromosomal architecture. Length of head, $h = 8$, and three genes per chromosomes were employed. The fourth step is to choose the linking function. The linking function must be chosen as "addition" or "multiplication" for algebraic sub trees (Ferreira 2002). Here, the sub trees were linked by addition. The fifth and final step is to choose the genetic operators. The parameters used per run are summarized as follows:

Number of chromosomes: 30, head size: 8, number of genes: 3, linking function: addition, fitness function error type: RRSE, mutation rate: 0.044, inversion rate: 0.1, one-point recombination rate: 0.3, two-point recombination rate: 0.3, gene recombination rate: 0.1, gene transposition rate: 0.1, insertion sequence transposition rate: 0.1, root insertion sequence transposition: 0.1.

2.3. Adaptive neuro-fuzzy inference system

ANFIS was first introduced by Jang (1993), Jang and Sun (1995) and Jang et al. (1997), and later on widely applied in engineering problems. Jang (1993) introduced architecture and a learning procedure for the FIS that uses a neural network learning algorithm for constructing a set of fuzzy IF-THEN rules with appropriate MFs from the specified input–output pairs. This procedure is called an adaptive neuro (i.e. neural network)-based fuzzy inference system (ANFIS). ANFIS learning employs the following two methods for updating membership function parameters: (1) back propagation for all parameters (using a steepest descent method); (2) a hybrid method consisting of back propagation for the parameters associated with the input membership and least squares estimation for the parameters associated with the output MFs. Specifically the ANFIS system of interest here is functionally equivalent to the Sugeno first-order fuzzy model (Jang et al. 1997). Detailed information for ANFIS can be found in Jang (1993).

2.4. Artificial neural networks

An ANN has one or more hidden layers, whose computational nodes are correspondingly called hidden neurons. The hidden neurons intervene between the external input and the network output in some useful manner. The network is enabled to extract higher order statistics by adding one or more hidden layers. In a rather loose sense, despite its local connectivity due to the extra set of synaptic connections and the extra dimension of network interconnections, the ANN acquires a global perspective. The detailed theoretical information about ANN can be found in Haykin (1998).

The ANN was trained using Levenberg–Marquardt (LM) technique because of the fact that this technique is more powerful and faster than the conventional gradient descent technique (Hagan and Menhaj 1994). The basic concept of the LM algorithm can be found in Kisi (2004). The ANN can have more than one hidden layers; however, theoretical works have shown that a single hidden layer is enough for an ANN to approximate any complex nonlinear function (Cybenco 1989). Therefore, in this study, one-hidden-layer ANN was used and the numbers of hidden layer neurons were found using a simple trial and error method in all applications. Sigmoidal and linear functions were used as the activation functions for the hidden and output nodes, respectively.

2.5. Wavelet–gene expression programming model

The wavelet–gene expression programming (WGEP) model, which was obtained combining two methods, DWT and GEP, is a GEP model which uses sub-time series components obtained using DWT on original data. For the WGEP model inputs, the

Table 1. The statistical parameters of the applied streamflow data.

	Daily data (m^3/s)			Monthly data (m^3/s)		
	Training data	Testing data	Whole data	Training data	Testing data	Whole data
X_{mean}	22.55	25.14	23.21	27.17	22.16	25.94
X_{min}	0.9	1.68	0.91	2.6	1.0	1.0
X_{max}	413	595	595	147.5	135.6	147.5
C_{sx}	3.87	5.8	4.64	1.8	2.31	1.89
S_d	33.02	39.9	34.87	28.79	27.68	28.57
C_v	1.46	1.58	1.51	1.06	1.25	1.1

original time series are decomposed into a certain number of sub-time series components (Ds) by Mallat DWT algorithm (Mallat 1989). The WGEP is constructed in which the Ds of original input time series are input of the GEP and the original output time series are output of the GEP. In the study, the current and previous streamflow time series were decomposed into various Ds at different resolution levels using DWT to forecast 1–3 days/month ahead streamflow values.

3. Applications

3.1. Used data

The daily and monthly streamflow values of the Karabuk station (station no: 1314) on the Filyos River in the Western Black Sea region of Turkey are used in the study. The observed daily data are 16 years (5840 days) long with an observation period between 1986 and 2001, while the monthly observed data are available for a longer time period (39 years), between 1964 and 2001. For each daily and monthly data sample, the first 75% of whole data were employed for developing of the applied models, while the remaining data were reserved for testing. Therefore, in daily observational data, the records from January 1986 to December 1997 were applied for training and the data from January 1988 to December 2001 were used for testing the models. Also the monthly data from January 1964 to June 1992 were employed for training, while the testing data set includes the observations from July 1992 to December 2001. Related information for the applied data set is presented in Table 1. In the table, the terms X_{mean}, X_{min}, X_{max}, C_{sx}, S_d, and C_v denote the mean, minimum, maximum, skewness, standard deviation, and coefficient of variation, respectively. From the table, it is clear that the daily streamflow data show high skewed distribution than monthly data.

3.2. Performance evaluation indices

Four statistical evaluation criteria were used to assess the model performance:

(1) the coefficient of correlation (R), which ranges between 0 and 1, with higher values indicate the better performance of the model. Legates and McCabe (1999) argued that this indicator should not be applied as fitness measure alone. Therefore, it is appropriate to quantify the error in the same unit as for the variables, as discussed by Legates and McCabe (1999). In this way, one may apply *RMSE* and *MAE*, defined as follows.

(2) the root-mean-square error (*RMSE*) defined as:

$$RMSE = \sqrt{\frac{1}{n}\sum_{i=1}^{n}\left(Q_{io} - Q_{ie}\right)^2} \tag{9}$$

where Q_{io} and Q_{ie} denote the observed and forecasted streamflow values.

(3) the mean absolute error (*MAE*) defined as:

$$MAE = \frac{\sum_{i=1}^{n}\left|Q_{ie} - Q_{io}\right|}{n} \tag{10}$$

(4) the variance account for (*VAF*) is defined as:

$$VAF = \left[1 - \frac{\mathrm{Var}(Q_{io} - Q_{ie})}{\mathrm{Var}(Q_{io})}\right] \times 100 \tag{11}$$

If the *VAF* is 100, this represents the perfect fit. A combined use of the aforementioned statistical measures can provide a good insight about the applied models.

4. Results and discussions

4.1. Wavelet decomposition of the observed daily and monthly streamflow time series

For the daily and monthly streamflows, four and three resolution levels were, respectively, employed in this study. Four resolution levels of sub-time series components (details) indicating (2^1 – day mode, 2^2 – day mode, 2^3 – day mode which is nearly weekly mode, and 2^4 – day mode which is nearly semi monthly mode), three resolution levels of sub-time series components indicating (2^1 – month mode, 2^2 – month mode, and 2^3 – month mode) and one approximation signal were, respectively, employed for the daily and monthly streamflows in this study. The approximate signal indicates the trend (low frequency) of the original streamflow time series while the details show high frequency.

Table 2 gives the correlation coefficients between each D sub-time series and original streamflow time series for the daily and monthly periods, respectively. In this table, the D_t and Q_{t+1} denotes the D sub-time series at time t and measured streamflow at time $t + 1$, respectively. As an example, the −0.081 indicates the correlation value between the $D1$ sub-time series at time t ($D1_t$) and the measured streamflow at time $t + 1$, Q_{t+1}. Thus, the $D1_t$, $D2_t$, … denote the sub-time series of the Q_t and vice versa. The correlation values given in Table 2 provide information for the determination of effective wavelet components on streamflow. It can be seen from the table that $D1$ component shows the lowest correlations for the daily and monthly periods. $D4$ and $D3$ components have the highest correlations for the daily and monthly periods, respectively. According to these correlation analyses between Ds and original current streamflow data (output), the $D1$ component was eliminated and $D2$, $D3$, and $D4$ components were selected. For the WGEP model, the new series obtained by adding the

Table 2. The correlation coefficients between each of sub-time series and streamflow data.

	Correlations			
Discrete wavelet components	D_t/Q_{t+1}	D_{t-1}/Q_{t+1}	D_{t-2}/Q_{t+1}	D_{t-3}/Q_{t+1}
Daily				
D1	−0.081	−0.070	0.067	0.027
D2	0.122	−0.018	−0.114	−0.047
D3	0.323	0.047	−0.194	−0.302
D4	0.329	0.302	0.261	0.201
Approximate	0.826	0.823	0.815	0.805
Monthly				
D1	−0.102	−0.066	0.027	0.016
D2	0.160	−0.230	−0.306	−0.075
D3	0.630	0.343	−0.034	−0.348
Approximate	0.198	0.176	0.187	0.189

effective *D*s components (*D*2, *D*3, and *D*4 for daily streamflows and *D*2 and *D*3 for monthly streamflows) and approximation component were used as inputs to the GEP model.

4.2. Streamflow forecasting

All the models, viz. GEP, ANFIS, ANN, and ARMA models were implemented using the recorded streamflow data at Karabuk station on the Filyos River in Turkey. This study examined various combinations of the previously recorded streamflow data (as inputs for GEP, ANFIS, and ANN models) to evaluate the degree of the effect of each of these variables on three time steps ahead streamflow values, as well as inter-comparison of the obtained results. It is relevant to note here that this study includes two parts as follows: Part 1 in which various combinations of streamflow data were applied as inputs for GEP, ANFIS, ANN, and ARMA models, and Part 2 in which the results produced using the same input combinations as Part1, but by applying DWT coefficients as GEP inputs. The GeneXpro software was applied to GEP implementation using streamflow data. Also two different program codes, including fuzzy logic and ANN toolboxes, were written in MATLAB language for the ANFIS and ANN simulations.

4.2.1. Part 1. Application of GEP, ANFIS, ANN, and ARMA models

In the first part of the study, various GEP, ANFIS, ANN, and ARMA models were developed using the recorded streamflow values. In this way, the evaluated input combinations were as follows:

(1) Q_t (GEP1, ANFIS1, ANN1)
(2) Q_{t-1}, Q_t (GEP2, ANFIS2, ANN2)
(3) Q_{t-2}, Q_{t-1}, Q_t (GEP3, ANFIS3, ANN3)
(4) Q_{t-3}, Q_{t-2}, Q_{t-1}, Q_t (GEP4, ANFIS4, ANN4)

where the Q_i denotes the streamflow value at time i (daily as well as monthly time scale). Having developed the mentioned input combination, the streamflow values at three time intervals (i.e., Q_{t+1}, Q_{t+2}, Q_{t+3}) were forecasted in both daily and monthly time scales using the applied models. Table 3 gives the final architectures of ANFIS and ANN models. The second column indicates the number of MFs of each input variable of ANFIS models. For instance, in the input combination (iv), the ANFIS model has 2, 2, 3, and 3 triangular MFs for the input variables, Q_{t-3}, Q_{t-2}, Q_{t-1}, and Q_t, respectively. There is not any basic rule to determine the number of MFs of ANFIS models and they are usually determined by trial and error. In selecting the number of MFs, a modeler should avoid using a large number of MFs or parameters to save time and calculation effort (Keskin et al. 2004). It should be noted that fuzzy MFs can take many forms, but triangular MFs are often selected for practical applications (Russel and Campbell 1996). However, recent investigations have shown that the type of MF does not affect the results significantly (Vernieuwe et al. 2005). The third column shows the number of input, hidden, and output nodes in each of the ANN models. Here, the optimal hidden layer nodes were also determined by trial and error method.

Table 4 gives the correlation coefficient (*R*), *RMSE*, *VAF*, and *MAE* values for daily GEP models during the testing period in all three forecasting intervals. The table clearly shows that the GEP model can produce better results for 1-day ahead forecast than those of 2- and 3-day ahead predictions. However, no satisfactory results were produced through using the GEP model for streamflow forecasting. Similarly, the results of application of ANFIS and ANN models for predicting daily streamflow in the same forecasting intervals as for GEP are summarized in Tables 5 and 6. From these tables, it can be seen that the performance of the all applied models are the same, with minor differences. The Akaike information criterion (AIC), first proposed by Akaike (1974), was used for selecting the optimal ARMA (p, q) models. The AIC is

$$\mathrm{AIC}(k) = N \ln(\mathrm{MSE}) + 2k \tag{12}$$

where N is the number of data points, and k is the number of free parameters used in the ARMA model. Listed in the upper part of the Table 7, show the statistical performance of the optimal ARMA models during the test period. Although the ARMA models produce some accurate results for predicting daily streamflow values for 1-day ahead time step, the results produced by ARMA for 2- and 3-day ahead are inferior to the results of GEP, ANFIS, and ANN models. In overall, all of the applied models have some better results for 1-day ahead prediction intervals than those produced for 2- and 3-days ahead intervals. Figure 1 displays the observed and forecasted daily streamflow values for the best models of 1-day ahead predictions through the scatterplots, during the testing period. The scatterplots in the figure clearly reveal that ARMA model can produce better results than those of the GEP, ANFIS, and ANN models for 1-day ahead streamflow prediction. However, as can be seen from the Tables 4–7, the accuracy of the ARMA model in forecasting 2- and 3-day ahead streamflow values are inferior to the other applied models. This can be obviously seen from the scatterplots in Figures 2 and 3. Among the AI methods, the ANFIS forecasts 2-day ahead streamflows better than the GEP and ANN. However, the ANN outperforms the ANFIS and GEP in forecasting 3-day ahead streamflow values. This

Table 3. Final structure of the ANFIS and ANN models.

	ANFIS structure (the number of MFs of each variable)	ANN structure (the number of input, hidden and output nodes)	
Model inputs	Daily and monthly models	Daily	Monthly
Forecast interval 1: Q_{t+1}			
Q_t	3	1, 1, 1	1, 4, 1
Q_{t-1}, Q_t	3, 3	1, 1, 1	1, 1, 1
Q_{t-2}, Q_{t-1}, Q_t	2, 2, 2	1, 2, 1	1, 5, 1
Q_{t-3}, Q_{t-2}, Q_{t-1}, Q_t	2, 2, 3, 3	1, 3, 1	1, 2, 1
Forecast interval 2: Q_{t+2}			
Q_t	3	1, 4, 1	1, 3, 1
Q_{t-1}, Q_t	2, 2	1, 8, 1	1, 2, 1
Q_{t-2}, Q_{t-1}, Q_t	2, 2, 3	1, 1, 1	1, 4, 1
Q_{t-3}, Q_{t-2}, Q_{t-1}, Q_t	2, 2, 3, 3	1, 5, 1	1, 6, 1
Forecast interval 3: Q_{t+3}			
Q_t	2	1, 5, 1	1, 9, 1
Q_{t-1}, Q_t	2, 3	1, 1, 1	1, 2, 1
Q_{t-2}, Q_{t-1}, Q_t	2, 3, 3	1, 1, 1	1, 8, 1
Q_{t-3}, Q_{t-2}, Q_{t-1}, Q_t	2, 2, 2, 2	1, 4, 1	1, 8, 1

Table 4. The results of GEP models for daily streamflow predictions during the test period.

	R	*RMSE* (m^3/s)	*VAF* (%)	*MAE* (m^3/s)
Input combinations	*Forecast interval 1:* Q_{t+1}			
Q_t	0.926	14.98	85.89	4.08
Q_{t-1}, Q_t	0.934	14.17	87.37	4.3
Q_{t-2}, Q_{t-1}, Q_t	0.938	13.74	88.11	4.09
Q_{t-3}, Q_{t-2}, Q_{t-1}, Q_t	0.941	13.52	88.61	3.61
	Forecast interval 2: Q_{t+2}			
Q_t	0.793	23.16	66.26	6.76
Q_{t-1}, Q_t	0.827	22.42	68.36	7.05
Q_{t-2}, Q_{t-1}, Q_t	0.825	22.56	68.08	7.21
Q_{t-3}, Q_{t-2}, Q_{t-1}, Q_t	0.815	23.21	66.14	7.06
	Forecast interval 3: Q_{t+3}			
Q_t	0.741	26.75	54.99	8.51
Q_{t-1}, Q_t	0.718	27.03	51.54	9.52
Q_{t-2}, Q_{t-1}, Q_t	0.742	26.67	55.27	8.68
Q_{t-3}, Q_{t-2}, Q_{t-1}, Q_t	0.723	27.54	52.28	9.48

Table 5. The results of ANFIS models for daily streamflow predictions during the test period.

	R	*RMSE* (m^3/s)	*VAF* (%)	*MAE* (m^3/s)
Input combinations	*Forecast interval 1:* Q_{t+1}			
Q_t	0.919	15.75	84.4	4.11
Q_{t-1}, Q_t	0.933	14.53	86.72	3.67
Q_{t-2}, Q_{t-1}, Q_t	0.938	13.94	87.77	3.63
Q_{t-3}, Q_{t-2}, Q_{t-1}, Q_t	0.825	24.73	61.51	4.65
	Forecast interval 2: Q_{t+2}			
Q_t	0.810	23.37	65.65	6.82
Q_{t-1}, Q_t	0.830	22.29	68.74	6.48
Q_{t-2}, Q_{t-1}, Q_t	0.902	17.17	81.44	6.14
Q_{t-3}, Q_{t-2}, Q_{t-1}, Q_t	0.814	29.72	66.38	6.67
	Forecast interval 3: Q_{t+3}			
Q_t	0.728	27.31	53.09	8.79
Q_{t-1}, Q_t	0.728	27.32	53.17	8.54
Q_{t-2}, Q_{t-1}, Q_t	0.739	26.83	54.72	8.55
Q_{t-3}, Q_{t-2}, Q_{t-1}, Q_t	0.739	26.85	54.65	8.69

confirms the results given in Tables 4–6. Tables 8–10 represent the results of the application of GEP, ANFIS, and ANN models for predicting monthly streamflows during the test period. Also the lower part of the Table 7 lists the results of ARMA model for predicting monthly streamflows. From the comparison of these results, it can be concluded that all of the applied models show weak results for predicting monthly (long term) streamflow values, especially for 2- and 3-month ahead predictions. Meanwhile, the ANN model surpasses the other models in all three prediction intervals with relatively lower *RMSE* and *MAE* values as well as with higher *R* and *VAF* values. The AI methods perform better than the ARMA models in forecasting monthly streamflows. Figures 4–6 illustrate the scatterplots of the observed and forecasted daily streamflow values for the optimal models of 1-, 2- and 3-day ahead predictions, during the testing period. It can be clearly seen from these figures that the ARMA model is inferior to the AI models. Of the AI models, the ANN performs better than the GEP and ANFIS models. Comparison of daily (Tables 4–6 and Figures 1–3) and monthly (Tables 8–10 and Figures 4–6) forecasts of the AI methods shows that the models provide much better estimates in daily time scale than those of the monthly time scale.

Table 6. The results of ANN models for daily streamflow predictions during the test period.

Input combinations	*R*	*RMSE* (m^3/s)	*VAF* (%)	*MAE* (m^3/s)
			Forecast interval 1: Q_{t+1}	
Q_t	0.924	15.32	85.22	4.05
Q_{t-1}, Q_t	0.941	13.66	88.26	3.55
Q_{t-2}, Q_{t-1}, Q_t	0.940	13.67	88.24	3.63
Q_{t-3}, Q_{t-2}, Q_{t-1}, Q_t	0.937	14.00	87.67	3.70
			Forecast interval 2: Q_{t+2}	
Q_t	0.816	23.09	66.48	6.71
Q_{t-1}, Q_t	0.837	21.87	69.92	6.32
Q_{t-2}, Q_{t-1}, Q_t	0.828	22.43	68.37	6.37
Q_{t-3}, Q_{t-2}, Q_{t-1}, Q_t	0.833	22.12	69.25	6.25
			Forecast interval 3: Q_{t+3}	
Q_t	0.736	26.99	54.20	8.60
Q_{t-1}, Q_t	0.750	26.41	56.16	8.29
Q_{t-2}, Q_{t-1}, Q_t	0.749	26.43	56.10	8.36
Q_{t-3}, Q_{t-2}, Q_{t-1}, Q_t	0.759	25.97	57.62	8.25

Table 7. The results of ARMA models for daily/monthly streamflow predictions during the test period.

	R	*RMSE* (m^3/s)	*VAF* (%)	*MAE* (m^3/s)
Daily stream flow prediction				
			Forecast interval 1: Q_{t+1}	
ARMA (3,2)	0.943	13.43	88.66	3.43
			Forecast interval 2: Q_{t+2}	
ARMA (3,2)	0.815	23.55	65.20	6.27
			Forecast interval 3: Q_{t+3}	
ARMA (3,2)	0.709	28.94	47.67	8.27
Monthly stream flow prediction				
			Forecast interval 1: Q_{t+1}	
ARMA (3,2)	0.615	23.34	37.27	15.06
			Forecast interval 2: Q_{t+2}	
ARMA (3,2)	0.380	27.63	13.95	17.36
			Forecast interval 3: Q_{t+3}	
ARMA (3,2)	0.385	27.70	14.83	17.87

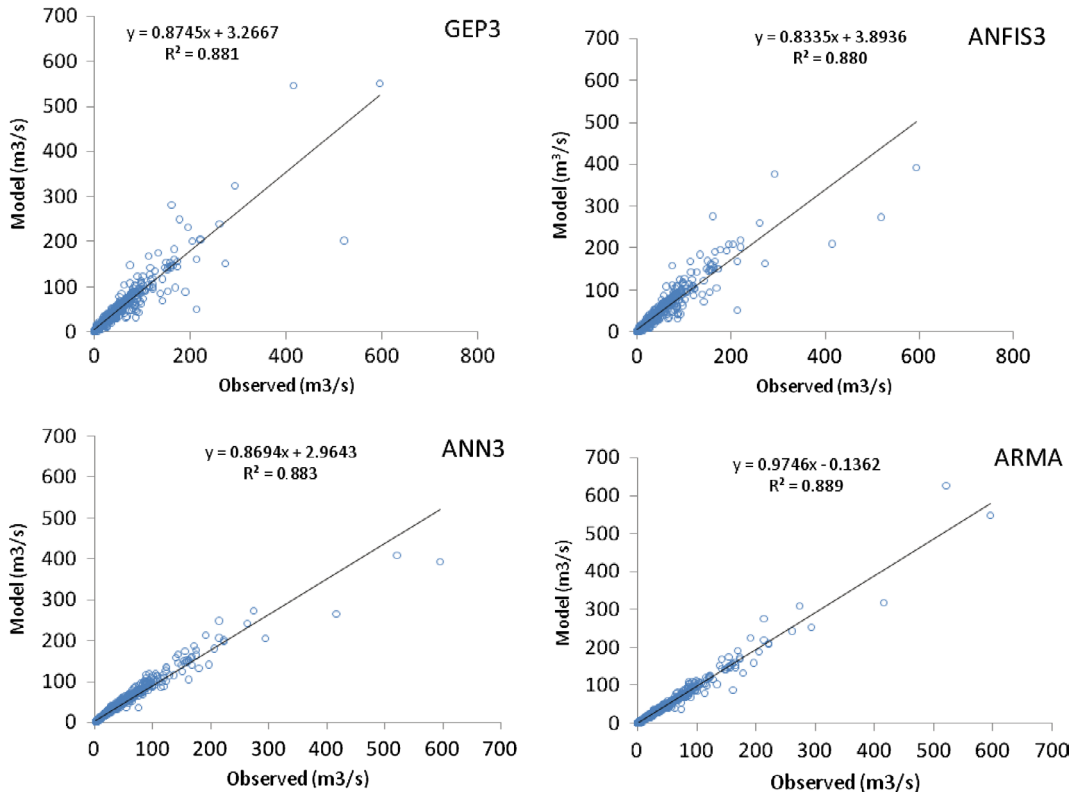

Figure 1. The observed and predicted streamflow values using the applied models for 1-day prediction interval.

The main reason behind this may be the fact that the number of monthly data is much less than the number of daily data. This causes underachievement of the data-driven AI models in learning behavior of the monthly streamflows.

4.2.2. Part 2. Application of hybrid wavelet–GEP model

In the second part of the study, wavelet–GEP (WGEP) combination model was evaluated to forecast streamflows in daily and monthly forecast horizons. In similarity of the previous

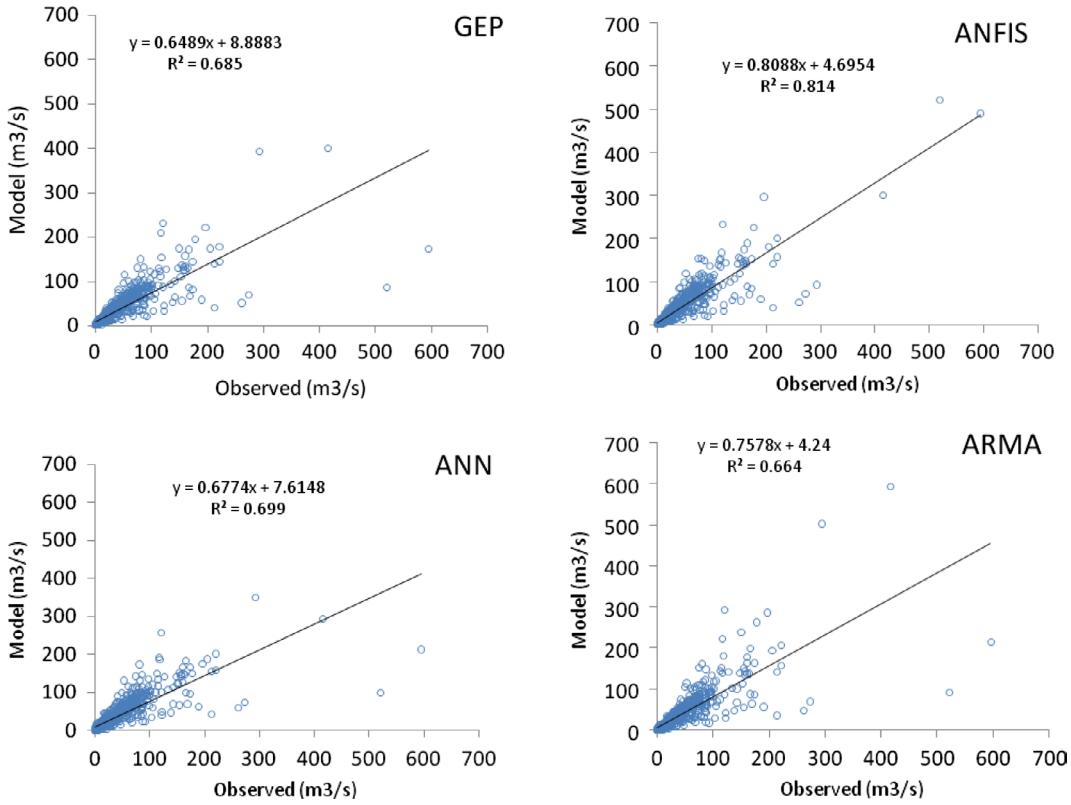

Figure 2. The observed and predicted streamflow values using the applied models for 2-day prediction interval.

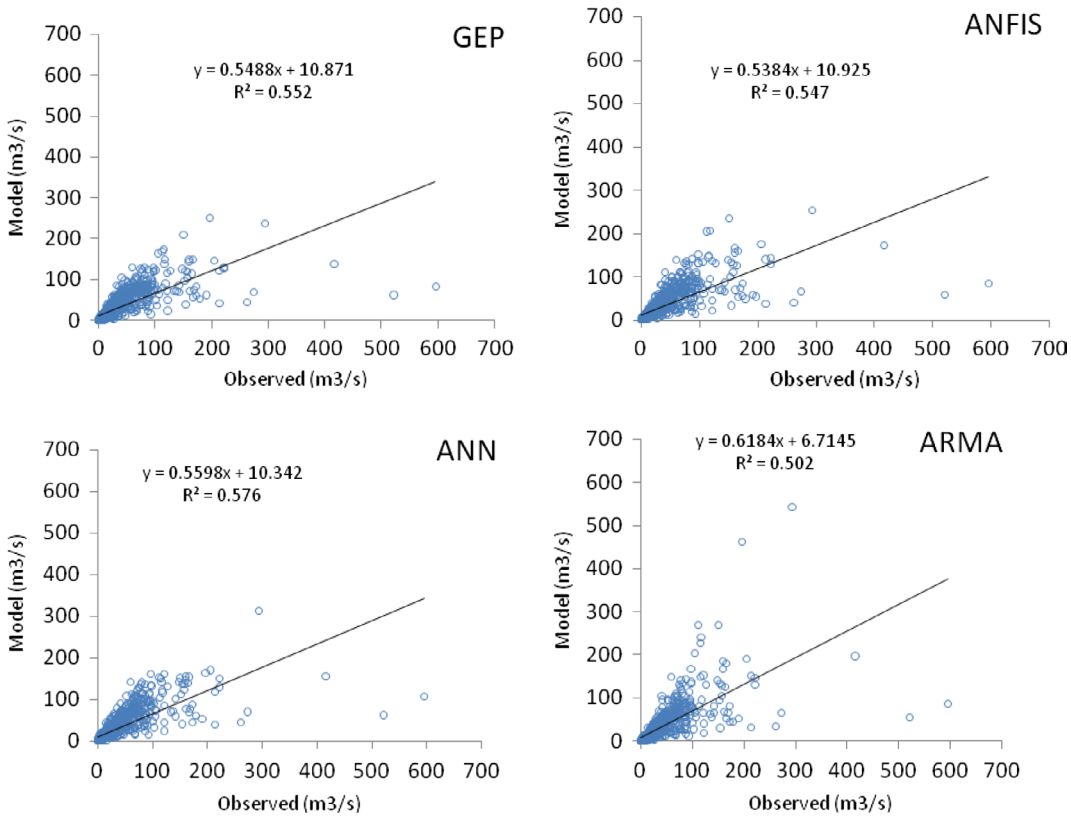

Figure 3. The observed and predicted streamflow values using the applied models for 3-day prediction interval.

section, too, the applied data set were divided into training and testing periods and three new WGEP models (for each prediction interval) were evaluated to forecast daily and monthly streamflows, as described before. Table 11 gives the statistical analysis of the WGEP results during the test period. As can be seen from the table, the WGEP4 model (corresponded to the input combination (iv)) surpasses the single, double, and triple-input WGEP models in forecasting streamflow values for all three prediction intervals, with relatively high correlation and *VAF* and low error (*RMSE* and *MAE*) values. For 1-day ahead

Table 8. The results of GEP models for monthly streamflow predictions during the test period.

	R	*RMSE* (m^3/s)	*VAF* (%)	*MAE* (m^3/s)
Input combinations			*Forecast interval 1:* Q_{t+1}	
Q_t	0.613	21.95	37.07	13.93
Q_{t-1}, Q_t	0.677	20.42	45.59	12.78
Q_{t-2}, Q_{t-1}, Q_t	0.695	25.78	14.76	13.75
$Q_{t-3}, Q_{t-2}, Q_{t-1}, Q_t$	0.672	20.64	44.58	13.07
			Forecast interval 2: Q_{t+2}	
Q_t	0.346	26.21	11.89	18.59
Q_{t-1}, Q_t	0.441	25.18	19.59	17.20
Q_{t-2}, Q_{t-1}, Q_t	0.347	26.76	8.21	18.93
$Q_{t-3}, Q_{t-2}, Q_{t-1}, Q_t$	0.360	27.94	2.74	20.12
			Forecast interval 3: Q_{t+3}	
Q_t	0.230	27.25	5.32	20.36
Q_{t-1}, Q_t	0.399	26.53	13.98	20.17
Q_{t-2}, Q_{t-1}, Q_t	0.168	26.55	10.57	18.29
$Q_{t-3}, Q_{t-2}, Q_{t-1}, Q_t$	0.145	29.45	9.57	19.2

Table 9. The results of ANFIS models for monthly streamflow predictions during the test period.

	R^2	*RMSE* (m^3/s)	*VAF* (%)	*MAE* (m^3/s)
Input combinations			*Forecast interval 1:* Q_{t+1}	
Q_t	0.611	21.93	37.16	13.82
Q_{t-1}, Q_t	0.692	20.06	47.56	12.54
Q_{t-2}, Q_{t-1}, Q_t	0.711	19.83	49.13	12.31
$Q_{t-3}, Q_{t-2}, Q_{t-1}, Q_t$	0.674	20.94	42.97	13.31
			Forecast interval 2: Q_{t+2}	
Q_t	0.263	26.85	6.94	19.5
Q_{t-1}, Q_t	0.409	24.45	16.71	17.64
Q_{t-2}, Q_{t-1}, Q_t	0.476	24.79	21.69	17.69
$Q_{t-3}, Q_{t-2}, Q_{t-1}, Q_t$	0.271	38.45	−79.97	23.25
			Forecast interval 3: Q_{t+3}	
Q_t	0.185	27.62	3.44	21.22
Q_{t-1}, Q_t	0.209	27.82	3.67	21.53
Q_{t-2}, Q_{t-1}, Q_t	0.271	27.82	4.35	21.61
$Q_{t-3}, Q_{t-2}, Q_{t-1}, Q_t$	0.114	42.50	2.11	28.54

Table 10. The results of ANN models for monthly streamflow predictions during the test period.

	R	*RMSE* (m^3/s)	*VAF* (%)	*MAE* (m^3/s)
Input combinations			*Forecast interval 1:* Q_{t+1}	
Q_t	0.670	20.74	44.10	13.30
Q_{t-1}, Q_t	0.646	21.19	41.28	13.81
Q_{t-2}, Q_{t-1}, Q_t	0.722	19.69	49.98	12.82
$Q_{t-3}, Q_{t-2}, Q_{t-1}, Q_t$	0.685	20.67	44.97	13.09
			Forecast interval 2: Q_{t+2}	
Q_t	0.368	25.96	13.40	18.22
Q_{t-1}, Q_t	0.487	24.47	22.35	17.09
Q_{t-2}, Q_{t-1}, Q_t	0.570	23.96	30.89	16.94
$Q_{t-3}, Q_{t-2}, Q_{t-1}, Q_t$	0.555	24.81	23.09	15.53
			Forecast interval 3: Q_{t+3}	
Q_t	0.348	26.52	10.90	19.54
Q_{t-1}, Q_t	0.471	25.75	16.66	18.82
Q_{t-2}, Q_{t-1}, Q_t	0.534	25.44	20.92	17.46
$Q_{t-3}, Q_{t-2}, Q_{t-1}, Q_t$	0.544	25.58	20.75	17.16

forecast, the WGEP4 model gives the most accurate results with a *R* value of 0.985, *RMSE* value of 6.85 (m^3/s), *MAE* value of 2.84 (m^3/s), and *VAF* value of 97.1; which outperforms the GEP, ANFIS, ANN, and ARMA models in streamflow forecasting (see Tables 4–7). For 2- and 3-day ahead forecast, the superiority of WGEP model to the other applied models increases and WGEP can be ranked as the best model for forecasting daily streamflow, based on the (DWT coefficients of) previously recorded streamflow values. Figure 7 shows the observed and modeled daily streamflow values (produced by WGEP) for all three time intervals. From the figures, it is clear that the WGEP predictions are close to the observed values with high correlations. From the best fit straight line equations (assume the equation as $y = a_0x + a_1$) in the scatterplots, it is clear that the coefficients a_0 and a_1 of WGEP models are close to the 1 and 0, respectively, which exhibits the high accuracy of WGEP model in forecasting daily streamflow values.

One of the strong points of using genetic programming (i.e., GEP) over other data-driven techniques (such as ANFIS and ANN) is that it produces explicit formulations (i.e., model expression) of the relationship that rules the physical phenomenon. Although ANFIS can produce some formulation between inputs and output using TS formulation, this includes lots of linear equations which are not explicit and cannot be interpreted easily. Such expressions produced by GEP may be subjected to some physical interpretations. In this way, one may discover knowledge using GEP, find some confirmation of the well-known physical relationships and evolve interesting new

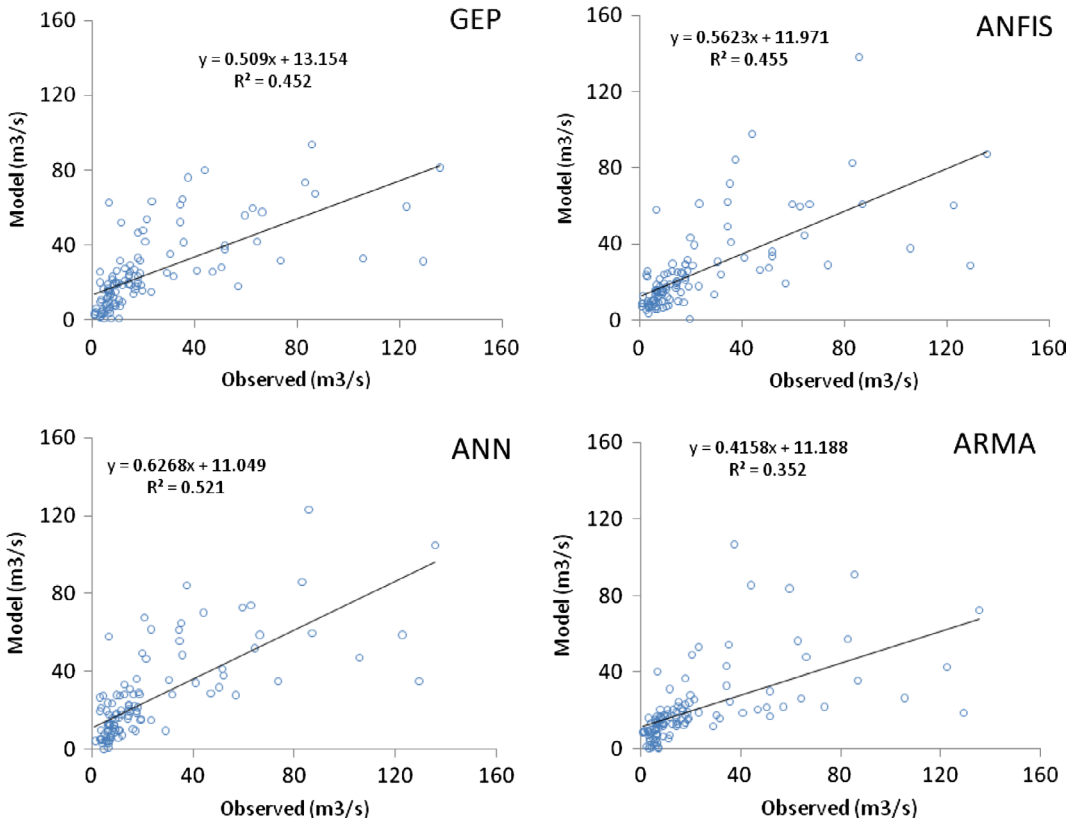

Figure 4. The observed and predicted streamflow values using the applied models for 1-month prediction interval.

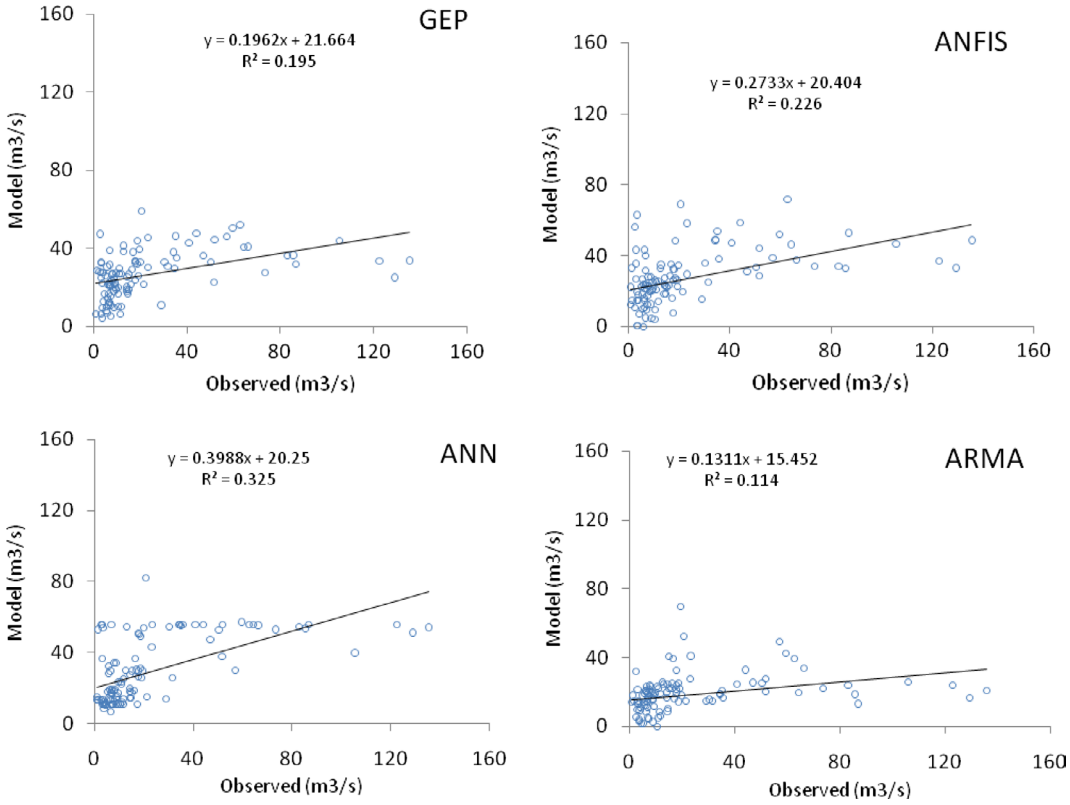

Figure 5. The observed and predicted streamflow values using the applied models for 2-month prediction interval.

formulae, as an upgradation of the particular cases of study. The mathematical expression of the quadruple-input WGEP model (WGEP4 model) for 1-day ahead forecast is shown in Figure 8 which actually is as follows:

$$Q_{t+1} = (d(0) - d(1)) + d(0) + ((d(3) - d(1))/(((d(2) + d(2))/d(3)) + (G_3 C_0^{(1.0/3.0)})))$$

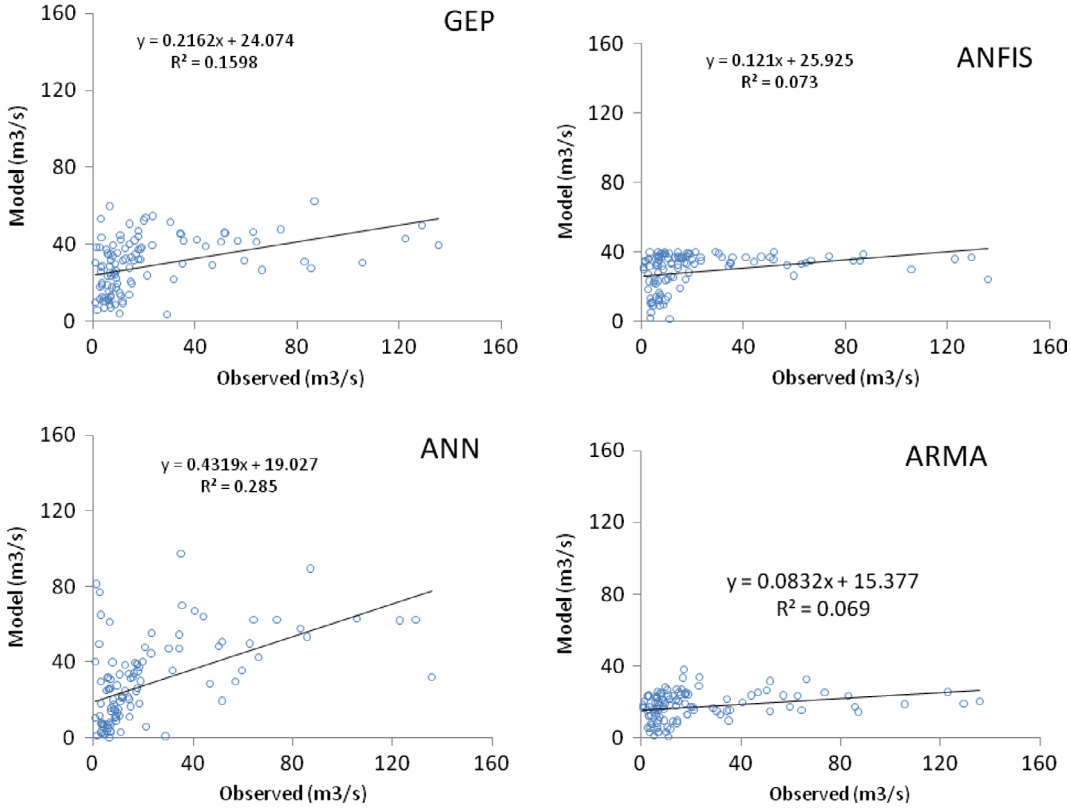

Figure 6. The observed and predicted streamflow values using the applied models for 3-month prediction interval.

Table 11. Error statistics of WGEP models for daily streamflow predictions during the test period.

	R	*RMSE* (m^3/s)	*VAF* (%)	*MAE* (m^3/s)
Input combinations		*Forecast interval 1:* Q_{t+1}		
DW_t	0.944	13.07	89.25	4.28
DW_{t-1}, DW_t	0.967	10.15	93.51	3.57
DW_{t-2}, DW_{t-1}, DW_t	0.969	9.74	94.02	3.37
$DW_{t-3}, DW_{t-2}, DW_{t-1}, DW_t$	0.985	6.85	97.1	2.84
		Forecast interval 2: Q_{t+2}		
DW_t	0.873	19.61	75.82	5.97
DW_{t-1}, DW_t	0.940	13.73	88.15	5.23
DW_{t-2}, DW_{t-1}, DW_t	0.950	12.92	89.51	4.58
$DW_{t-3}, DW_{t-2}, DW_{t-1}, DW_t$	0.977	8.33	95.63	3.72
		Forecast interval 3: Q_{t+3}		
DW_t	0.808	23.56	65.08	7.71
DW_{t-1}, DW_t	0.849	21.1	71.99	7.33
DW_{t-2}, DW_{t-1}, DW_t	0.878	19.8	75.33	6.17
$DW_{t-3}, DW_{t-2}, DW_{t-1}, DW_t$	0.906	15.67	81.85	5.71

where $d(0) = Q_t$, $d(1) = Q_{t-1}$, $d(2) = Q_{t-2}$ and $d(3) = Q_{t-3}$; and $G3C0 = 5.62$

After putting the corresponding values, the equation becomes

$$Q_{t+1} = (2Q_t - Q_{t-1}) + \left(\frac{Q_{t-3} - Q_{t-1}}{\frac{2Q_{t-2}}{Q_{t-3}} + 1.78} \right) \quad (13)$$

Table 12 represents the statistical analysis of the WGEP model for modeling monthly streamflows. From the table, it can be clearly seen that the proposed WGEP model can model monthly streamflows in all three time intervals with relatively high correlation and low error values. Unlike the daily streamflow simulations (where the quadruple-input models gave the best results among other input combinations), the triple-input WGEP models could produce the best results among other models. For the simulations of monthly streamflows from 1- to 3-months ahead forecast intervals, the WGEP accuracy is influenced as follows: *R* and *VAF* decrease from 0.834 and 69.72 (for 1-month ahead) to 0.732 and 51.27 (for 3-month ahead), respectively; whereas *RMSE* and *MAE* increase from 15.3 and 10.95 m^3/s (for 1-month ahead) to 19.32 and 14.68 m^3/s (for 3-month ahead), respectively. The comparison of the WGEP model with other data-driven approaches (as has been listed through Tables 7–10) demonstrates that the new WGEP combination model surpasses all of the other applied models, with much better results. The observed and modeled monthly streamflow values obtained by WGEP are shown in Figure 9 for all three time intervals. Comparison of Figure 9 with Figures 4–6 clearly indicates that the WGEP predictions are much closer to the observed values than those of the GEP, ANFIS, ANN, and ARMA models. The mathematical expression of the triple-input WGEP model for 1-month ahead forecast is as follows:

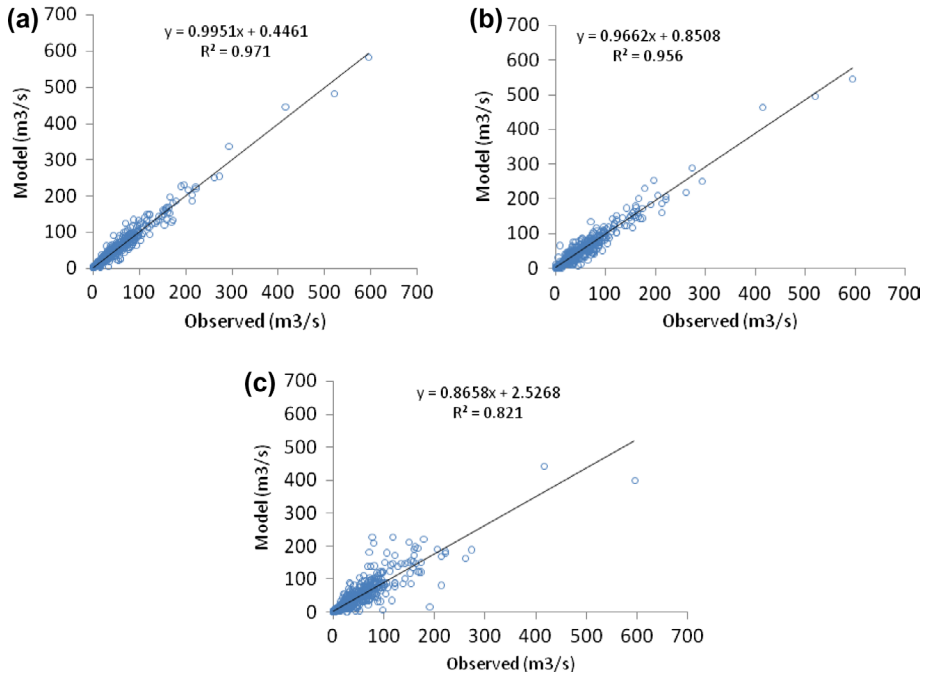

Figure 7. The observed and predicted streamflow values using WGEP model for (a) 1-day, (b) 2-day, and (c) 3-day ahead prediction intervals.

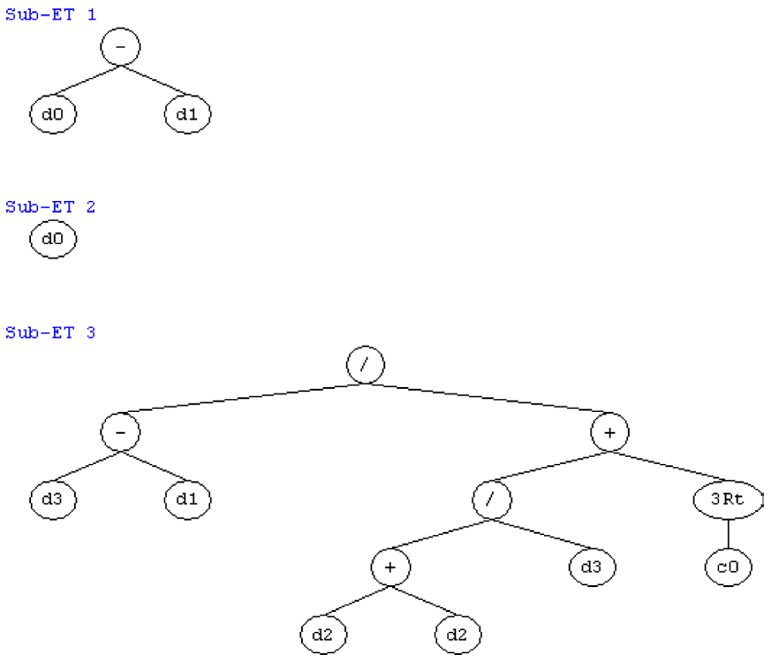

Figure 8. The tree expression of the WGEP4 model for 1-day ahead forecast.

Table 12. Error statistics of WGEP models for monthly streamflow predictions during the test period.

	R	*RMSE* (m^3/s)	*VAF* (%)	*MAE* (m^3/s)
Input combinations		*Forecast interval 1:* Q_{t+1}		
DW_t	0.714	19.40	51.03	13.01
DW_{t-1}, DW_t	0.824	16.16	65.73	10.86
DW_{t-2}, DW_{t-1}, DW_t	0.834	15.3	69.72	10.95
DW_{t-3}, DW_{t-2}, DW_{t-1}, DW_t	0.833	15.42	69.09	10.53
		Forecast interval 2: Q_{t+2}		
DW_t	0.470	24.67	21.72	17.79
DW_{t-1}, DW_t	0.774	17.88	59.46	13.79
DW_{t-2}, DW_{t-1}, DW_t	0.786	17.42	61.82	13.04
DW_{t-3}, DW_{t-2}, DW_{t-1}, DW_t	0.771	18.32	56.42	14.85
		Forecast interval 3: Q_{t+3}		
DW_t	0.161	27.66	2.49	21.33
DW_{t-1}, DW_t	0.656	21.51	41.55	17.27
DW_{t-2}, DW_{t-1}, DW_t	0.733	19.32	51.27	14.68
DW_{t-3}, DW_{t-2}, DW_{t-1}, DW_t	0.698	20.29	78.06	16.02

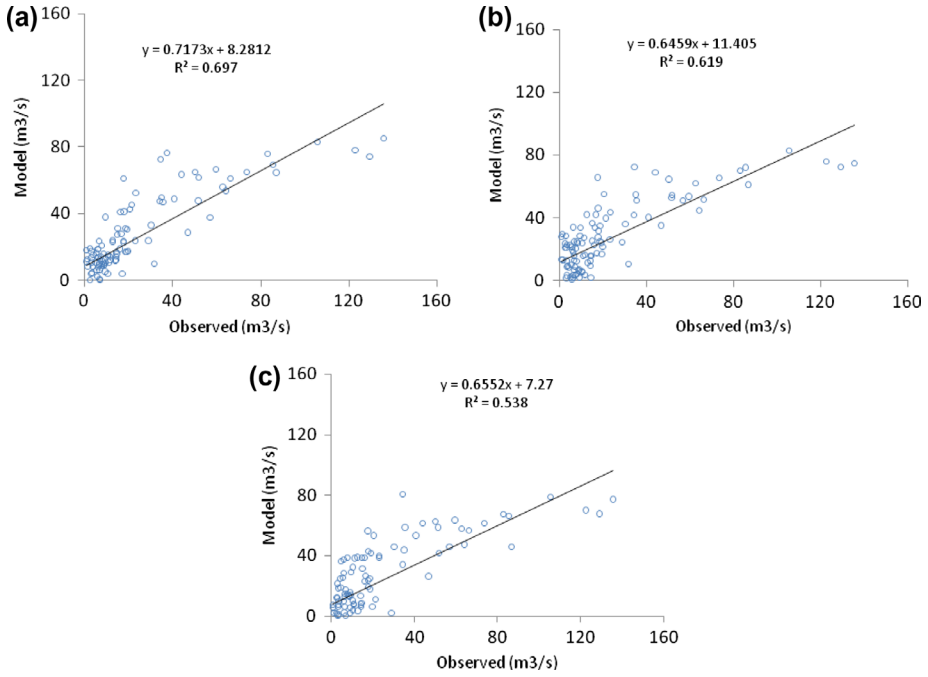

Figure 9. The observed and predicted streamflow values using WGEP model for (a) 1-month, (b) 2-month, and (c) 3-month ahead prediction intervals.

Table 13. Analysis of variance for streamflow forecast during the test period.

Method	Daily		Monthly	
	F-statistic	Resultant significance level	*F*-statistic	Resultant significance level
Forecast interval 1: Q_{t+1}				
WGEP	0.048	0.827	0.293	0.589
GEP	0.006	0.938	0.379	0.539
ANFIS	0.044	0.833	0.506	0.478
ANN	0.052	0.819	0.555	0.457
ARMA	0.279	0.598	0.406	0.525
Forecast interval 2: Q_{t+2}				
WGEP	$1.5.10^{-7}$	0.999	1.052	0.0306
GEP	0.002	0.964	1.798	0.181
ANFIS	0.006	0.936	1.882	0.171
ANN	0.136	0.712	4.500	0.035
ARMA	1.688	0.194	1.917	0.168
Forecast interval 3: Q_{t+3}				
WGEP	0.326	0.568	0.012	0.915
GEP	0.133	0.715	1.979	0.161
ANFIS	0.279	0.597	4.840	0.029
ANN	0.314	0.575	3.577	0.060
ARMA	4.325	0.038	3.224	0.074

$$Q_{t+1} = \mathrm{Exp}\left[1.42 - arctg\left(Q_t - 8.9\right)\right] + \mathrm{Exp}\left\{arctg\left[Q_{t-1} - \sin\left(\frac{\mathrm{Exp}\ Q_{t-1}}{Q_{t-1}}\right)\right]\right\} + 2Q_t - Q_{t-1} + 0.325\ Q_{t-2} \quad (14)$$

The comparison of the Equations (12) and (13) shows that the WGEP model for predicting 1-month ahead streamflows is more complicated than 1-day ahead streamflow forecast model, although the input parameters of the latter is more than the former. A reason behind this may be the complications accompanied with monthly streamflow forecasting.

The results were also tested using one way analysis of variance for verifying the robustness (the significance of differences between the model estimates and observed values) of the models. Both tests are set at a 95% significant level. The statistics of the test are given in Table 13. In long-term (monthly) streamflow forecasting case, the WGEP models yielded smaller testing values with higher significance levels than those of the other models (GEP, ANFIS, ANN, ARMA). According to the test results, the WGEP seems to be more robust (the similarity between the observed monthly streamflows and WGEP estimates are high) in monthly streamflow prediction than the others. In short-term (daily) streamflow forecasting case, the GEP, WGEP, and ANFIS forecasts seem to be the most robust than those of the other models for the 1-, 2-, and 3-day ahead forecast intervals.

5. Conclusion

The ability of WGEP combination models for predicting short-term and long-term streamflows has been investigated in this study. In the first part of the study, various GEP, ANFIS, ANN, and ARMA models were developed using the recorded daily and monthly streamflows. Although the ARMA models produced some accurate results for predicting daily streamflow values for 1-day ahead time step, the results produced by ARMA for 2- and 3-day ahead were found to be inferior to the results of GEP, ANFIS, and ANN models. Among the AI methods, the ANFIS predicted 2-day ahead streamflows better than the GEP and ANN models. However, the ANN outperformed the ANFIS and GEP in forecasting 3-day ahead streamflows. In monthly streamflow forecasting case, the GEP, ANFIS, and ANN models showed better accuracy than those of the ARMA models. Of the AI models, the ANN performed better than the GEP and ANFIS models for predicting 1-, 2-, and 3-month ahead streamflows.

In the second part of the study, WGEP combination model was evaluated to predict streamflows in daily and monthly forecast horizons. In 1-, 2-, and 3-day ahead (short-term) forecasting case, the WGEP models performed much better than the GEP, ANFIS, ANN, and ARMA models in streamflow forecasting. Increasing forecast horizon does not terribly deteriorate the WGEP accuracy. This is not the same for GEP, ANFIS, ANN, and ARMA models. In case of forecasting 1-, 2-, and 3-month ahead (long-term) streamflows, the proposed WGEP modeled monthly streamflows in all three time intervals with relatively high correlation and low error values.

Disclosure statement

No potential conflict of interest was reported by the authors.

References

Akaike, H. (1974). "A new look at the statistical model identification." *IEEE Trans. Autom. Control*, AC-19, 716–723.

ASCE Task Committee on Application of Artificial Neural Networks in Hydrology. (2000a). "Artificial neural networks in hydrology, I: preliminary concepts." *ASCE J. Hydrologic Eng.*, 5(2), 115–123.

ASCE Task Committee on Application of Artificial Neural Networks in Hydrology. (2000b). "Artificial neural networks in hydrology, II: hydrological applications." *ASCE J. Hydrologic Eng.*, 5(2), 124–137.

Banzhaf, W., Nordin, P., Keller, P.E., and Francone, F.D. (1998). *Genetic programming*, Morgan Kaufmann, San Francisco, CA, 512 pp.

Coulibaly, P., Anctil, F., Aravena, R., and Bobee, B. (2001). "Artificial neural network modeling of water table depth fluctuations." *Water Resour. Res.*, 37(4), 885–896.

Coulibaly, P., and Burn, H.D. (2004). "Wavelet analysis of variability in annual Canadian streamflows." *Water Resour. Res.*, 40, W03105–W03118.

Cybenco, G. (1989). "Approximation by superpositions of a sigmoidal function." *Math Control Signals Syst.*, 2, 303–314.

Ferreira, C. (2001). "Gene expression programming: a new adaptive algorithm for solving problems." *Complex Syst.*, 13(2), 87–129.

Ferreira, C. (2002).Gene expression programming in problem solving. Part VI, In: Soft Computing and Industry, 635–653.

Ferreira, C. (2006). *Gene expression programming: mathematical modeling by an artificial intelligence*, 2nd ed., Berlin-Heidelberg, Springer-Verlag.

Goldberg, D.E. (1989). *Genetic algorithms in search, optimization, and machine learning*. Addison –Wesley, Reading, MA, 432 pp.

Hagan, M.T., and Menhaj, M.B. (1994). "Training feed forward networks with the Marquaradt algorithm." *IEEE Trans. Neural Netw.*, 6, 861–867.

Haykin, S. (1998). *Neural networks – a comprehensive foundation*, 2nd ed., Prentice-Hall, Upper Saddle River, NJ, 26–32.

Huang, W., Xu, B., and Chan-Hilton, A. (2004). "Forecasting flows in Apalachicola river using neural networks." *Hydrol. Processes*, 18, 2545–2564.

Jain, A., and Kumar, A.M. (2007). "Hybrid neural network models for hydrologic time series forecasting." *Appl. Soft Comput.*, 7, 585–592.

Jang, J.S.R. (1993). "ANFIS: adaptive-network-based fuzzy inference system." *IEEE Trans. Syst. Man and Cybern.*, 23(3), 665–685.

Jang, J.S.R., and Sun, C.T. (1995). "Neuro fuzzy modeling and control." *Proc. IEEE*, 83, 378–406.

Jang, J.S.R., Sun, C.T., and Mizutani, E. (1997). *Neurofuzzy and soft computing: a computational approach to learning and machine intelligence*, Prentice-Hall, NJ.

Keskin, M.E., Terzi, O., and Taylan, D. (2004). "Fuzzy logic model approaches to daily pan evaporation estimation in western Turkey." *Hydrol. Sci. J.*, 49(6), 1001–1010.

Kisi, O. (2004). "Multi layer perceptions with Levenberg–Marquardt training algorithm for suspended sediment concentration prediction and estimation." *Hydrol. Sci. J.*, 40, 1025–1040.

Kişi, Ö. (2006a). "Generalized regression neural networks for evapotranspiration modeling." *Hydrol. Sci. J.*, 51(6), 1092–1105.

Kişi, Ö. (2006b). "Evapotranspiration estimation using feed forward neural networks." *Nordic Hydrol.*, 37(3), 247–260.

Kisi, O. (2007a). "Streamflow forecasting using different artificial neural network algorithms." *J. Hydrol. Eng.*, 12(5), 532–539.

Kişi, Ö. (2007b). "Evapotranspiration modeling from climate data using a neural computing technique." *Hydrol. Processes*, 21(6), 1925–1934.

Kisi, O. (2008). "River flow forecasting and estimation using different artificial neural network techniques." *Hydrol. Res.*, 39(1), 27–40.

Kisi, O. (2009). "Neural networks and wavelet conjunction model for intermittent streamflow forecasting." *J. Hydrol. Eng.*, 14(8), 773–782.

Kisi, O., and Shir, J. (2011). "Precipitation forecasting using wavelet-genetic programming and wavelet-neuro-fuzzy conjunction models." *Water Resour. Manage.*, 25(13), 3135–3152.

Kisi, O., and Shiri, J. (2012). "Wavelet and neuro-fuzzy conjunction model for predicting water table depth fluctuations." *Hydrol. Res.*, 43(3), 286–300.

Koza, J.R. (1992). *Genetic programming: on the programming of computers by means of natural selection*, The MIT Press, Cambridge, MA, 840 pp.

Labat, D. (2005). "Recent advances in wavelet analyses: part 1. A review of concepts." *J. Hydrol.*, 314(1–4), 275–288.

Labat, D., Ronchail, J., and Guyot, J.L. (2005). "Recent advances in wavelet analyses: part 2 – amazon, parana, orinoco and congo discharges time scale variability." *J. Hydrol.*, 314(1–4), 289–311.

Legates, D.R., and McCabe, G.J. (1999). "Evaluating the use of goodness-of-fit measures in hydrologic and hydroclimatic model validation." *Water Resour. Res.*, 35(1), 233–241.

Lu, R.Y. (2002). "Decomposition of interdecadal and interannual components for North China rainfall in rainy season." *Chin. J. Atmos.*, (in Chinese) 26, 611–624.

Maier, H.R., and Dany, G.C. (2000). "Neural networks for the prediction and forecasting of water resources variables: a review of modelling issues and applications." *Environ. Model. Softw.*, 15, 101–124.

Mallat, S.G. (1989). "A theory for multiresolution signal decomposition: the wavelet representation." *IEEE Trans. Pattern Anal. Mach. Intell.*, 11(7), 674–693.

Mamdani, E.H., and Assilian, S. (1975). "An experiment in linguistic synthesis with a fuzzy logic controller." *Int. J. Man Mach. Stud.*, 7(1), 1–13.

Minnes, A.W., and Hall, M.J. (1996). "Artificial neural networks as rainfall-runoff models." *Hydrol. Sci. J.*, 41(3), 399–417.

Nayak, P.C., Sudheer, K.P., Rangan, D.M., and Ramasastri, K.S. (2004). "A neuro-fuzzy computing technique for modeling hydrological time series." *J. Hydrol.*, 291, 52–66.

Nourani, V., and Andalib, G. (2015). "Daily and monthly suspended sediment load predictions using wavelet based artificial intelligence approaches." *J. Mountain Sci.*, 12(1), 85–100.

Partal, T., and Kisi, O. (2007). "Wavelet and neuro-fuzzy conjunction model for precipitation forecasting." *J. Hydrol.*, 342, 199–212.

Partal, T., and Küçük, M. (2006). "Long-term trend analysis using discrete wavelet components of annual precipitations measurements in Marmara region (Turkey)." *Phys. Chem. Earth*, 31, 1189–1200.

Russel, S.O., and Campbell, P.F. (1996). "Reservoir operating rules with fuzzy programming." *J. Water Resour. Planning Manage.*, 122(3), 165–170.

Shiri, J., and Kisi, O. (2010). "Short-term and long-term streamflow forecasting using a wavelet and neuro-fuzzy conjunction model." *J. Hydrol.*, 394, 486–493.

Shiri, J., and Kisi, O. (2011). "Application of artificial intelligence to estimate daily pan evaporation using available and estimated climatic data in the Khozestan Province (Southwestern Iran)." *J. Irrig. Drain. Eng.*, 137(7), 412–425.

Smith, L.C., Turcotte, D.L., and Isacks, B. (1998). "Stream flow characterization and feature detection using a discrete wavelet transform." *Hydrol. Processes*, 12, 233–249.

Supharatid, S. (2003). "Application of a neural network model in establishing a stage-discharge relationship for a tidal river." *Hydrol. Processes*, 17, 3085–3099.

Takagi, T., and Sugeno, M. (1985). "Fuzzy identification of systems and its application to modeling and control." *IEEE Trans. Syst. Man Cybern.*, 15(1), 116–132.

Tayfur, G. (2002). "Artificial neural networks for sheet sediment transport." *Hydrol. Sci. J.*, 4(6), 879–892.

Vernieuwe, H., Georgieva, O., De Baets, B., Pauwels, V.R.N., Verhoest, N.E.C., and De Troch, F.P. (2005). "Comparison of data-driven Takagi-Sugeno models of rainfall-discharge dynamics." *J. Hydrol.*, 302(1–4), 173–186.

Wang, W., and Ding, J. (2003). "Wavelet network model and its application to the prediction of the hydrology." *Nat. Sci.*, 1(1), 67–71.

Wang, W., Van Gelder, P.H.A.J.M., Vrijling, J.K., and Ma, J. (2006). "Forecasting daily streamflow using hybrid ANN models." *J. Hydrol.*, 324, 383–399.

Xingang, D., Ping, W., and Jifan, C. (2003). "Multiscale characteristics of the rainy season rainfall and interdecadal decaying of summer monsoon in North China." *Chin. Sci. Bull.*, 48, 2730–2734.

Zhou, H.C., Peng, Y., and Liang, G.-H. (2008). "The research of monthly discharge predictor-corrector model based on wavelet decomposition." *Water Resour. Manage.*, 22(2), 217–227.